New therapeutic targets in the intrinsic apoptotic pathway in neuroblastoma

Lamers, Fieke

Publication date
2012


Apoptosis
C
CASP3
C
BAX
BAX
BAX
BCL2

4

Targeted BCL2 Inhibition Effectively Inhibits Neuroblastoma Tumor Growth

Targeted BCL2 Inhibition Effectively Inhibits Neuroblastoma Tumor Growth

Fieke Lamers[1], Linda Schild[1], Ilona J.M. den Hartog[1] Marli E. Ebus[1], Ellen M. Westerhout[1], Ingrid Øra[2], Jan Koster[1], Rogier Versteeg[1], Huib N. Caron[3], Jan J. Molenaar[1]

[1] Department of Oncogenomics, Academic Medical Center, University of Amsterdam, Meibergdreef 15, PO box 22700, 1105 AZ Amsterdam, The Netherlands.
[2] Department of Pediatric Oncology, Skåne University Hospital, Lund University, Lund, Sweden.
[3] Department of Pediatric Oncology, Emma Kinderziekenhuis, Academic Medical Center, University of Amsterdam, Meibergdreef 15, PO box 22700, 1105 AZ Amsterdam, the Netherlands

Abstract

Genomic aberrations of key regulators of the apoptotic pathway have hardly been identified in neuroblastoma. We detected high *BCL2* mRNA and protein levels in the majority of neuroblastoma tumors by Affymetrix expression profiling and Tissue Micro Array analysis. This *BCL2* mRNA expression is strongly elevated compared to normal tissues and other malignancies. Most neuroblastoma cell lines lack this high *BCL2* expression. Only two neuroblastoma cell lines (KCNR and SJNB12) show *BCL2* expression levels representative for neuroblastoma tumors. To validate *BCL2* as a therapeutic target in neuroblastoma we employed lentivirally mediated shRNA. Silencing of *BCL2* in KCNR and SJNB12 resulted in massive apoptosis, while cell lines with low *BCL2* expression were insensitive. Identical results were obtained by treatment of the neuroblastoma cell lines with the small molecule BCL2 inhibitor ABT263, which is currently being clinically evaluated. Combination assays of ABT263 with most classical cytostatics showed strong synergistic responses. Subcutaneous xenografts of a neuroblastoma cell line with high *BCL2* expression in NMRI nu/nu mice showed a strong response to ABT263. These findings establish BCL2 as a promising drug target in neuroblastoma and warrant further evaluation of ABT263 and other BCL2 inhibiting drugs.

Introduction

BCL2 is an anti-apoptotic member of the BCL2 family proteins.[1] When localized at the outer mitochondrial membrane it binds BAX and BAK resulting in inhibition of pore formation and prevention of cytosolic release of caspase-activating proteins.[1,2] *BCL2* was originally identified as a partner of t(14;18) translocations that occur in nearly all cases of follicular lymphoma and in some diffuse large B-cell lymphoma. Also amplification of *BCL2* is found in these malignancies.[3] *BCL2* transgenic mice are known to develop follicular lymphoma, indicating its oncogenic function.[4] Deregulation of other *BCL2* family members is found in several other tumor types and is correlated with therapy resistance.[1,2]. BCL2 inhibitors are in phase 1/2 clinical trials for several malignancies such as chronic lymphocytic leukemia, glioblastoma, small cell lung cancer and malignant melanoma, showing promising results.[1,5-7]

Neuroblastoma are pediatric tumors that originate from the embryonal precursor cells of the sympathetic nervous system. Despite extensive treatment, children with high stage neuroblastoma have a poor prognosis with 20 to 40% overall survival.[8-11] Genomic aberrations in genes directly involved in apoptotic signaling are rare in neuroblastoma. Deregulation seems to be caused by epigenetic events.[12,13] P53 is mostly intact in primary neuroblastoma although signaling has shown to be disturbed.[10] *CASP8 (Caspase 8)* is hypermethylated and thereby inactive in some neuroblastoma resulting in an inactive extrinsic apoptotic pathway.[10] And finally the inhibitor of apoptosis gene *BIRC5 (Survivin)* is highly expressed in neuroblastoma, which correlates to a poor prognosis.[14-16] None of these signaling proteins is currently a prime candidate for targeted inhibition. P53 inhibition by Nutlin has shown to be effective in neuroblastoma but clinical application awaits new generations of this type of compound.[17] Direct inhibitors of BIRC5 signaling are not available, but YM155, a transcriptional inhibitor of *BIRC5* has shown promising results in vitro and in vivo.[18-23] However, additional targets in the apoptotic pathway for which clinically applicable compounds are available are urgently needed.

The role of BCL2 family members in neuroblastoma has been subject of several studies. *BCL2* expression was reported to be strongly increased in developing sympathetic nervous system and was suggested to regulate survival during maturation.[24-26] Another member of the BCL2 family, *MCL1*, has been reported to mimic the BCL2 function and to circumvent the effects of BCL2 inhibition in neuroblastoma. Compounds that modulate both MCL1 and BCL2 were found to be

most effective in neuroblastoma cell lines and a profile of the pro-apoptotic members of the BCL2 family proteins can predict sensitivity of neuroblastoma cell lines to BCL2 inhibitors.[27,28]

Several inhibitors of BCL2 are currently in clinical trials.[5,12,13] G3139 is an antisense oligodeoxynucleotide targeting *BCL2* mRNA resulting in RNAse H activation. ABT263 is a small molecule mimetic of the BH3 domain of the pro-apoptotic BAD protein that is currently in clinical trial in chronic lymphatic leukemia.[29] ABT263 binds with high affinity to BCL2, BCLXL and BCLW resulting in inhibition of these proteins, but binds with a much lower affinity to MCL1 and BCL2A1[30] This BCL2 small molecule inhibitor has been studied in the Pediatric Preclinical drug Testing Program (PPTP) and was not found to be effective in five neuroblastoma in vivo tumor models.[31]

In this study we showed that most neuroblastoma tumors have high BCL2 expression, but most neuroblastoma cell lines lack BCL2. Targeted inhibition of *BCL2* by lentiviral shRNA resulted in massive apoptosis in two neuroblastoma cell lines with high BCL2 expression, but not in neuroblastoma cell lines with low or absent expression of *BCL2*. The small molecule BCL2 inhibitor ABT263 achieved the same results. Combination assays of ABT263 with most classical cytostatics showed strong synergistic responses. ABT263 showed anti-tumor efficacy in a neuroblastoma xenograft model. Our pre-clinical data package provides a strong rational for clinical development of ABT263 in neuroblastoma patients.

Methods

Patient Material

The neuroblastic tumor panel used for Affymetrix microarray analysis contains 88 neuroblastoma samples. All samples were derived from primary tumors obtained at diagnosis from patients treated at the Emma Childen's Hospital in Amsterdam from 1991. Material was obtained during surgery and immediately frozen in liquid nitrogen.

RNA extraction and Affymetrix profiling

For profiling total RNA of neuroblastoma cell lines and tumors was extracted using Trizol reagent (Invitrogen) according to the manufacturer's protocol. RNA concentration was determined using the NanoDrop ND-1000 and quality was

determined using the RNA 6000 Nano assay on the Agilent 2100 Bioanalyzer (Agilent Technologies). For Affymetrix Microarray analysis, fragmentation of RNA, labeling, hybridization to HG-U133 Plus 2.0 microarrays and scanning was carried out according to the manufacturer's protocol (Affymetrix Inc.). The expression data were normalized with the MAS5.0 algorithm within the GCOS program of Affymetrix. Target intensity was set to 100 (α1=0.04 and α2 0.06). If more than one probe set was available for one gene the probe set with the highest expression was selected, considered that the probe set was correctly located on the gene of interest. Mostly this is a probe set at the 3' end. Public available neuroblastoma datasets we used were of Delattre[32], Lastowska (geo ID: gse13136) and Speleman[33]. Public available datasets were used for comparing neuroblastoma with normal tissues (Roth dataset, geo ID: gse3526) and adult tumors (EXPO dataset, geo ID: gse2109). The data were analyzed with the R2 microarray analysis and visualization platform (http://r2.amc.nl).

Tissue array

Paraffin-embedded tumors were cut into 4-µm sections, mounted on aminoalkylsaline-coated glass slides, and dried overnight at 37°C. Sections were dewaxed in xylene and graded ethanol, and endogenous peroxidase was blocked in a 0.3% H2O2 solution in 100% methanol. Subsequently, the slides were rinsed thoroughly in distilled water and pretreated with a boiling procedure for 10 min in 10/1 mM Tris/EDTA pH 9 in an autoclave. After rinsing in distilled water and PBS, slides were incubated with primary antibody against BCL2 (M0887, DAKO). Slides were incubated for 1 hour in room temperature in a 1:100 solution (diluted in an antibody diluent). Slides were then blocked with a postantibody blocking (Power Vision kit, ImmunoLogic) 1:1 diluted in PBS for 15 minutes, followed by a 30-minute incubation with poly–horseradish peroxidase (HRP)–goat α mouse/rabbit IgG (Power Vision kit, ImmunoLogic) 1:1 diluted in PBS. Chromogen and substrate were 3,3′-diaminobenzidine (DAB) and peroxide (1% DAB and 1% peroxide in distilled water). Nuclear counterstaining was done with hematoxylin. After dewatering in graded ethanol and xylene, slides were coated with glass and evaluated independently by two observers. As a negative control we used liver tissue.

Cell lines

All cell lines were grown in Dulbecco Modified Eagle Medium (DMEM), supplemented with 10% fetal calf serum, 10 mM L-glutamine, 10 U/ml penicillin, Non Essential Amino Acids (1x) and 10 µg/ml streptomycin. Cells were maintained at 37 ˚C under

5% CO_2. For primary references of these cell lines, see Molenaar et al[34].

Lentiviral shRNA production and transduction

Lentiviral particles were produced in HEK293T cells by cotransfection of lentiviral vector containing the short hairpin RNA (shRNA) with lentiviral packaging plasmids pMD2G, pRRE and pRSV/REV using FuGene HD. Supernatant of the HEK293T cells was harvested at 48 and 72 hours after transfection, which was purified by filtration and ultracentrifuging. The concentration was determined by a p24 ELISA.

Cells were plated in a 10% confluence. After 24 hours cells were transduced with lentiviral BCL2 shRNA (Sigma, TRCN0000040069 and TRCN0000040071) in various concentrations (Multiplicity of infection (MOI): 1 – 3). SHC-002 shRNA (non-targeting shRNA: CAACAAGATGAAGAGCACCAA) was used as a negative control. 24 hours after transduction medium was refreshed and puromycin was added to determine the efficacy of transduction. Protein of floating and attached cells was harvested 72 hours after transduction and analyzed by Western blot. Nuclei were harvested 48 and 72 hours after transfection for FACS analysis.

Lentiviral over-expression clones

BCL2 and *MCL1* cDNA was obtained from a plasmid provided by addgene (plasmid 21605 and 8768:3336)[35,36] and cloned into pLenti4/TO/V5-Dest according to manufacturer's procedures (Invitrogen). The sequence has been checked using the manufacturer's primers (pL4-TO/V5 fwd and pL4-dest rev)

Compounds

ABT263 (Toronto Research Chemicals) was dissolved in DMSO in a stock concentration of 20 mM from which concentration series were made in medium from 0.001 to 100 µM. Other compounds used were obtained from Sigma-Aldrich. Stock solutions were made for Vincristin (10 mM in dH_2O), Etoposide (50 mM in DMSO), Cisplatin (50 mM in DMF) and doxorubicin (50 mM in dH_2O). Compound was added to the cells 24 hours after plating.

MTT-assay

Cells were plated in a 10-30% confluence in a 96-well plate and treated after 24 hours with ABT263 in a concentration range between 0.008 to 20 µM. 72 hours after treatment, 10 µl of Thyazolyl blue tetrazolium bromide (MTT, Sigma M2128) was added. After 4-6 hours of incubation 100 µl of 10% SDS, 0.01 M HCl was added to stop the reaction. The absorbance was measured at 570 nm and 720 nm using

a platereader (biotek). The IC50 (concentration drug needed for 50% cell viability reduction) was calculated using concentration vector curves. For synergy assays ABT263 was combined with doxorubicin, cisplatin, vincristin or etoposide in a 96-well plate format. 24 hours after plating the cells in a 10-30% confluence, both compounds were added at the same time. All experiments were performed multiple times in duplo. The Combination Index (CI) was calculated by the Chou Talalay method[37] using the CalcuSyn software.

Western Blotting

48 hours after treatment with ABT263, attached and floating cells were harvested on ice. Cells were lysated with Laemmlibuffer (20% glycerol, 4% SDS, 100mM Tris HCl pH 6.8 in mQ). Protein was quantified with RC-DC protein assay (Bio-Rad). Lysates were separated on a 10 % SDS-Page gel and electroblotted on a transfer membrane (Millipore, IPFL00010). Blocking and incubation were performed in OBB according to manufacturer's protocol (LI-COR). Primary antibodies used were BCL2 rabbit polyclonal (cell signaling, #2872), PARP rabbit polyclonal (cell signaling, #9542), Cytochrome C mouse monoclonal (BD Pharmingen, 556433) and β-actin mouse monoclonal (abcam, ab6276). The secondary antibodies used were provided by LI-COR. Proteins were visualized with the Odyssey bioanalyzer (LI-COR).

Cell fractionation

Protein of SJNB12 cells was harvested and fractionated using the Subcellular Proteome Extraction Kit according to manufacturer's protocol (Novagen, 539790). Fraction I (cytosol) and II (cell organelle) were used for Western blot

FACS analysis

72 hours after treatment with ABT263 both the attached and the floating cells were fixed with 100% ethanol at -20 ºC. After fixing, the cells were stained with 0.05 mg/ml propidium iodide and 0.05 mg/ml RNAse A in PBS. After 1 hour incubation, DNA content of the nuclei was analyzed using a fluorescence activated cell sorter. A total of 10,000 nuclei per sample were counted. The cell cycle distribution and apoptotic sub G1 fraction was determined using Flowjo.

Mouse model

The animal experiments were performed with permission and according to the standards of the Dutch committee for animal research ethics (DEC 101934). $2.5*10^6$ cells of KCNR were injected subcutaneously in both flanks of NMRI nu/nu mice.

Tumors were allowed to grow to 500 mm^3. One of these subcutaneous tumors was harvested and cut in pieces of 2 x 2 mm for subsequent subcutaneous transplantation in both flanks of the next generation mice. For the experiment we used 2 groups of 6 mice each and we started treatment 4 days after implantation of the tumors. One group was treated with ABT263 in a concentration of 100 mg/kg/day (in 100 µl 5% DMSO, 9.5% ethanol, 28.5% polyethylene glycol, 57% Phosal 50 PG) and the other group was treated with 100 µl of vehicle only for 21 days orally.

Results

BCL2 is over-expressed in most neuroblastoma tumors but only sporadic in cell lines

BCL2 family members are up-regulated in many kinds of cancer.[28] They include BCL2, MCL1, BCLXL, BCLW, BCLB and BFL1 and can be functionally redundant[1,38]. We therefore analyzed the expression of all family members in neuroblastoma tumors using Affymetrix expression data. *BCL2* is the only family member that shows a strong up-regulation in neuroblastoma tumors compared to other cancer types and compared to various normal tissues (fig 1a). The other anti-apoptotic BCL2 family members were equally or lower expressed in neuroblastoma compared to other tumors and normal tissues (suppl fig 1/2). To study the correlation between *BCL2* mRNA and protein expression in neuroblastoma, we performed tissue array analysis of 42 neuroblastoma tumors with 3 core biopsies per sample. All 42 tumors had cytoplasmic staining for BCL2 but a clear variation was visible (suppl fig 3). All tumors were scored and categorized into three groups. Low BCL2 protein expression was scored in 6 tumors whereas 14 tumors displayed intermediate and 22 tumors high BCL2 protein levels. Tumors with a high *BCL2* mRNA expression showed significantly higher BCL2 protein levels (fig 1b), indicating that *BCL2* mRNA levels are representative for BCL2 protein levels in neuroblastoma tumors.

Neuroblastoma cell lines have a much lower *BCL2* mRNA expression compared to neuroblastoma tumors (fig 1a). KCNR and SJNB12 were the only two cell lines with *BCL2* mRNA expression levels comparable to tumors. Western blot analysis of all cell lines in our panel revealed that, like in tumors, high *BCL2* mRNA levels correspond with high BCL2 protein levels (fig 1c). We conclude that only a few neuroblastoma cell lines are suited to study the effects of BCL2 inhibition in neuroblastoma.

To investigate whether high *BCL2* expression levels are related to genomic defects in

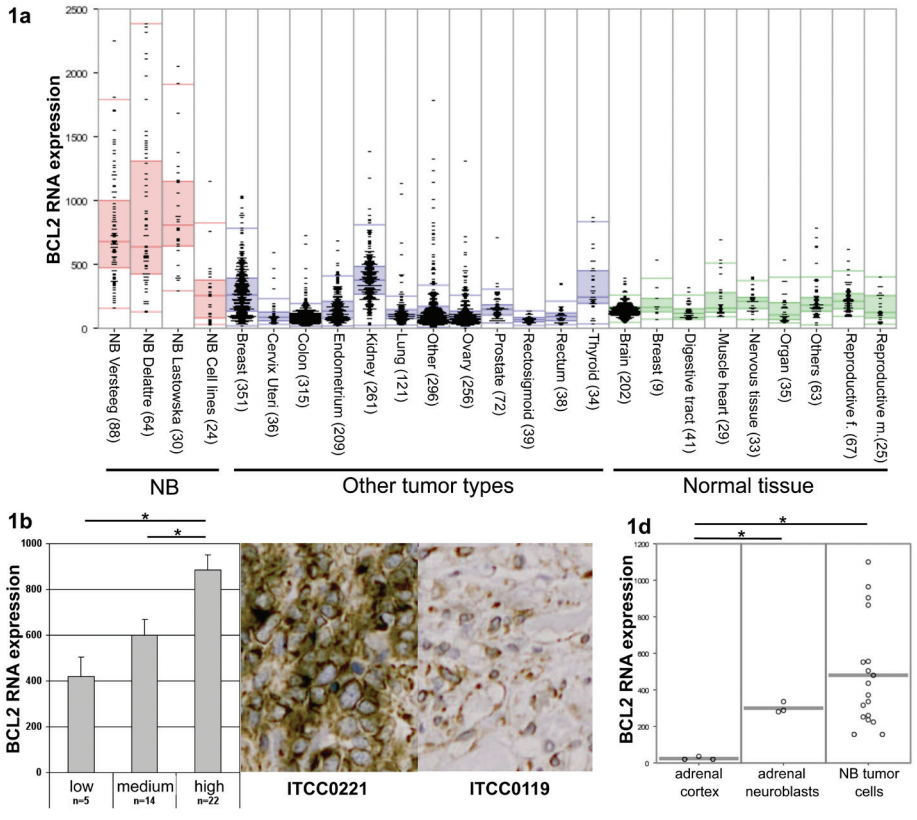

Figure 1: BCL2 expression in neuroblastoma tumors and cell lines (A) *BCL2* RNA expression data in Neuroblastoma tumors and cell lines (red), other tumors (blue) and normal tissue (green) based on Affymetrix profiling. In a combined boxdot-plot every dot represents one sample; the number of tumor samples is given between brackets. The colored boxes represent the area between the 25th and the 75th percentile with a line in between indicating the median. (B) Left: Correlation between Affymetrix *BCL2* RNA expression data (Y-axis) and BCL2 protein expression (3 expression groups are shown on the X-axis) based on a tissue array of the same tumors. Significance is indicated by *. Right: example of immunohistochemistry of a tumor with high BCL2 expression (ITCC0221) and low BCL2 expression (ITCC0119) (C) For all cell lines of the panel the *BCL2* RNA expression level based on Affymetrix profiling is represented. Red: >4x average (A), Orange: >2A <4A, Yellow: >0.5A <2A, Green: <0.5 A. Western blots of BCL2 expression in cell line panel were incubated with BCL2 and Actin antibodies. (D) *BCL2* RNA expression data in neuroblastoma tumor cells, adrenal neuroblasts and adrenal cortex. Every dot represents one sample. The line represents the average expression. Significance is indicated by *.

neuroblastoma, we analysed the *BCL2* locus on chromosome 18 in array CGH data of our neuroblastoma series. Whole chromosome 18 gain was detected in 15 out of 88 neuroblastoma tumors, but *BCL2* mRNA levels did not correlate to chr.18 gain (data not shown), suggesting that *BCL2* expression is transcriptionally regulated. To analyse whether high BCL2 expression is a property of the sympatho-adrenal lineage from which neuroblastoma are derived, we compared the *BCL2* mRNA expression of normal adrenal neuroblasts and tumors in a published series of de Preter et al.[33] and found no significant differences (fig 1d). This is in agreement with earlier immunohistochemical analyses[26], and suggests that high *BCL2* expression is a characteristic of the sympathetic adrenal lineage.

BCL2 silencing results in apoptosis in a subset of neuroblastoma cell lines

We selected five neuroblastoma cell lines with various *BCL2* expression levels, of which KCNR and SJNB12 have high expression, LAN5 and SKNBE have intermediate expression and SKNAS has low *BCL2* expression. In all cell lines *BCL2* was silenced using two lentiviral shRNAs, targeting different parts of the coding sequence. Western blot analysis showed a >80% decrease of BCL2 protein expression 72 hours after transduction in all cell lines with *BCL2* expression (fig 2a). *BCL2* silencing resulted in cell death 72 hours after transduction in the cell lines with high or intermediate *BCL2* expression as shown by PARP cleavage. SKNAS has no *BCL2* expression and did not show induction of PARP cleavage after treatment with the BCL2-specific shRNA vectors (fig 2a). The differences in phenotypic effect after *BCL2* silencing were confirmed using light microscopy (fig 2b) and MTT assays (fig 2c). Both assays showed a strong decrease of cell viability after silencing *BCL2* in cell lines with high expression of *BCL2* while SKNAS was completely insensitive. These findings suggest that *BCL2* is a potential target for therapy in neuroblastoma tumors with moderate to high expression of *BCL2*.

ABT263 induces apoptosis in NB cell lines with high expression of BCL2

The strong phenotypes induced by shRNA-mediated BCL2 inhibition urged us to test whether these results can also be achieved by a clinically applicable compound. ABT263 is a small molecule BCL2 inhibitor currently in clinical testing. We treated the same five neuroblastoma cell lines with ABT263. The results were strikingly similar to the phenotypes after *BCL2* shRNA treatment. The four cell lines with high or intermediate *BCL2* expression showed apoptotic cell death as indicated by Parp cleavage (fig 3a) and an increase in sub G1 fraction on FACS analysis (fig 3b, table 1), whereas SKNAS was completely insensitive for the compound at μM

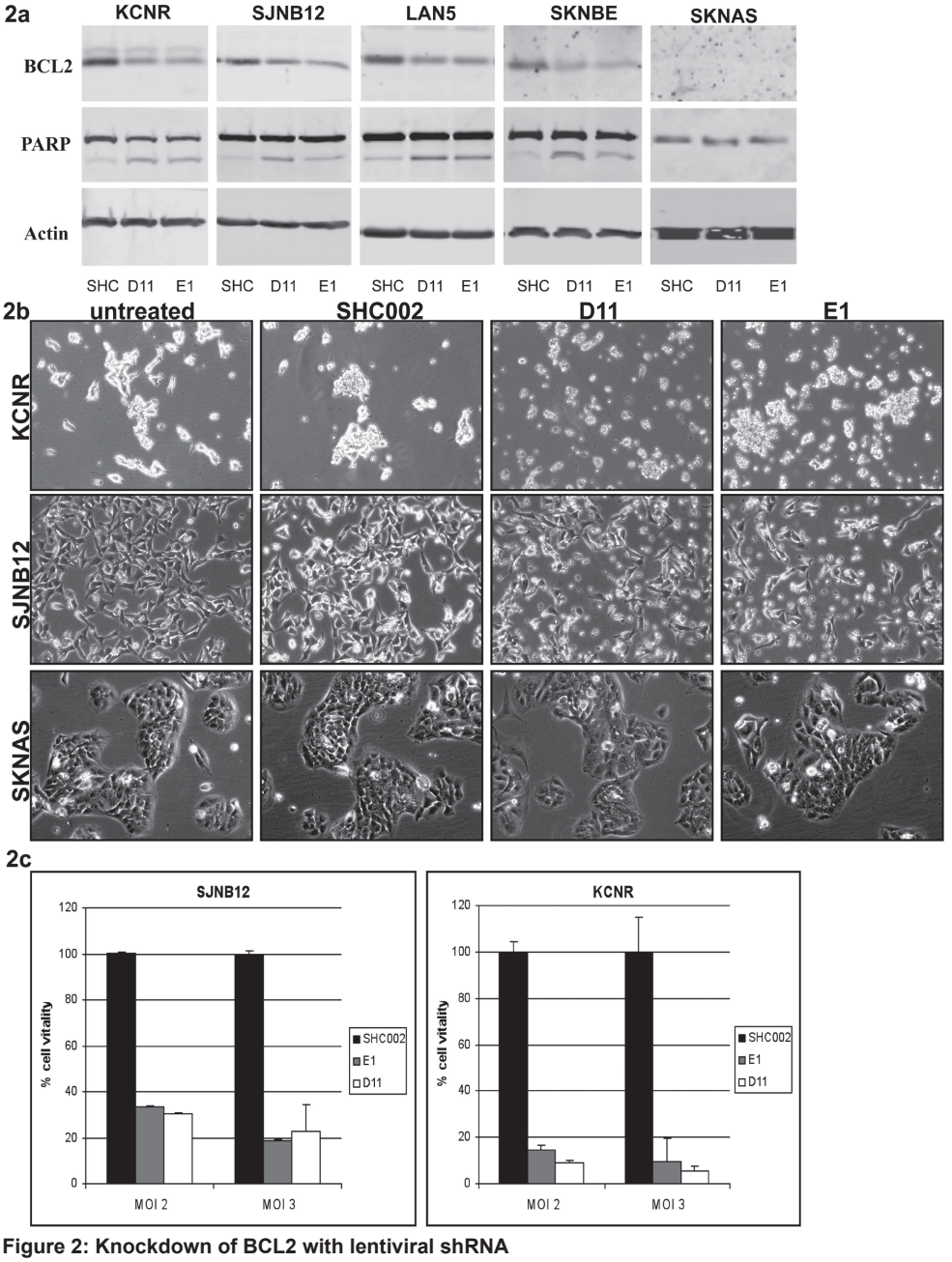

Figure 2: Knockdown of BCL2 with lentiviral shRNA

(A) Protein lysates were made of cells of Fig 2b. Western blot was performed and incubated with BCL2, PARP and Actin antibodies. (B) Pictures of the cells transduced with two different lentiviral BCL2 shRNAs were made 72 hours after transduction with a 100x magnitude. (C) MTT assay was performed 7 to 10 days after transduction with BCL2 shRNA. Cell viability is represented on the Y-axis and the multiplicity of infection (MOI) is represented on the X-axis.

ABT263 (uM)	sub G1 fraction(%)				
	KCNR	SJNB12	LAN5	SKNBE	SKNAS
0	14	16.1	4.3	10.2	2.2
0.008	19.7	14	*	*	*
0.04	19.1	18	*	*	*
0.2	31.7	28.6	30.5	*	*
1	41.2	32.1	40.7	14.5	2.6
5	55	37.6	42.5	19.7	3.7
10	*	*	36.2	22.5	3.3
15	*	*	40	22.5	4.1
20	*	*	*	28.9	5.5

Table 1. Apoptotic fraction after treatment with ABT263 in cell line panel
Percentage of the subG1 fraction as determined by FACS analysis.

concentrations and did not show induction of apoptosis (fig 3a-b). The concentration ABT263 required for 50% cell survival (IC50) was determined for all cell lines in our panel using MTT assays. The IC50 varied from 0.1 μM in KCNR to >100 μM in SKNAS (fig 3c) and showed an inverse correlation to the *BCL2* RNA expression (fig 3d).

These findings suggest that targeted inhibition of BCL2 by ABT263 leads to a similar response as targeted knock down of the *BCL2* mRNA. To further test the BCL2-inhibitory effect of ABT263, we performed a cell fractionation assay of neuroblastoma cells treated with ABT263. Western blot analysis showed at 24 h after treatment a strong transient increase of cytoplasmatic levels of Cytochrome C, which confirms mitochondrial release of Cytochrome C as a result of BCL2 inhibition (fig 3e).

ABT263 inhibits tumor growth in a neuroblastoma mouse model

The in vitro results of ABT263 urged us to test the compound in a neuroblastoma mouse model. We used serial transplants in NMRI Nu/Nu mice of xenografts of the human neuroblastoma cell line KCNR. Mice were treated orally with 100 mg/kg/day ABT263 for three weeks. After treatment, the mice were followed until they had to be terminated due to tumor volume. The ABT263-treated mice showed a strong delay in tumor growth and had a reduced tumor take. ABT263 induced a delay of 29 days on average compared to the DMSO-treated control mice (fig 4). In the ABT263 treated

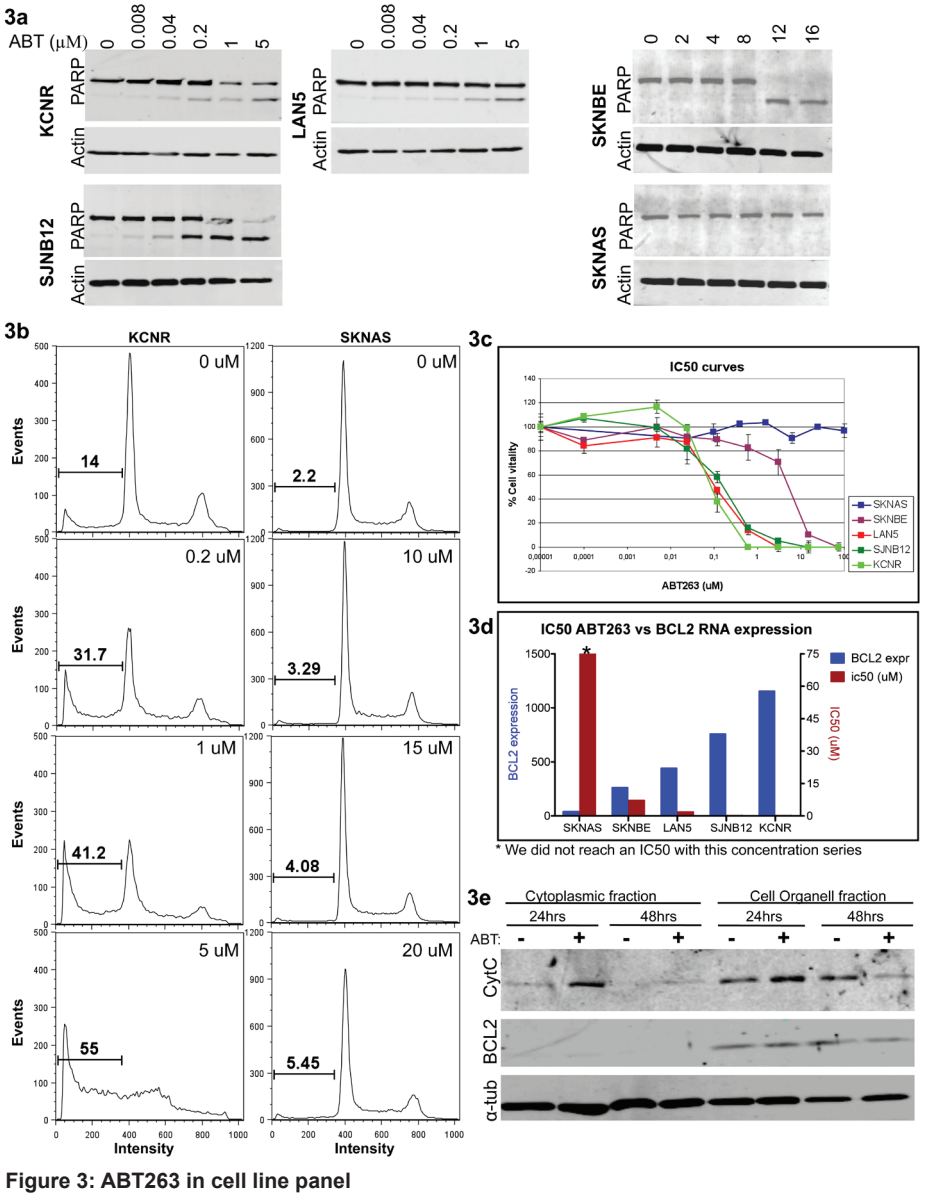

Figure 3: ABT263 in cell line panel

(A). Lysates were made of cells treated with ABT263. Western blots were incubated with PARP and Actin antibodies. (B) FACS analysis of cells treated with ABT263. The Y-axes of the graphs represent the number of events and the X-axes represent the size of the particles detected. Apoptosis is shown by the sub G1 fraction. (C) Cell viability curves of all cell lines of the panel after treatment with ABT263 as determined by an MTT-assay. Cell viability is represented on the Y-axis and the ABT263 concentration in μM is represented on the X-axis. (D) IC50 values of the cell lines tested for ABT263 that were calculated from the data in fig 3c are represented by the red bars. BCL2 RNA expression of these cell lines is shown by the blue bars. (E) Cell fractionation assay performed on SJNB12 cells treated with ABT263 for 24 hours. Blots were incubated with Cytochrome C, BCL2, and a-tubulin antibodies.

mice 5 tumors developed out of 12 tumors that were implanted, whereas in the DMSO treated group 9 out of 12 implants formed tumors. We conclude that ABT263 also in vivo shows a strong inhibitory effect on xenografts of a human neuroblastoma cell line with high *BCL2* expression.

Synergy between ABT263 and regular cytostatics

ABT263 potentiates an apoptotic response, suggesting that synergistic effects in combination with apoptosis inducing compounds might occur. In addition solid knowledge of combination treatment with classical cytostatics is a requisite for further clinical implementation of ABT263. We analyzed this in MTT synergy assays with the key compounds used in neuroblastoma treatment according to the DCOG NBL 2007 trial protocol. Doxorubicin, Vincristin and Etoposide showed strong synergistic responses with ABT263 in the two neuroblastoma cell lines SJNB12 and KCNR, which both have a high *BCL2* expression (table 2). ABT263 also showed synergy with cisplatin in SJNB12, but surprisingly an antagonistic effect with cisplatin in KCNR. As expected, no enhancement between ABT263 and the other compounds

	KCNR	SJNB12	SKNAS	F2112
doxorubicin	++++ (0.14)	++++ (0.19)	+ / -	+ / -
cisplatinum	- - - - - (>10)	+++ (0.58)	+ / -	+ / -
vincristine	+++ (0.51)	+++++ (<0.1)	+ / -	+ / -
etoposide	++++ (0.21)	+++++ (<0.1)	+ / -	+ / -

Table 2. Synergy assays

Combination Indexes for each cell line treated with ABT263 combined with each drug indicated are presented in this table. The degree of synergism is presented by + or -. +++++: very strong synergism; ++++: strong synergism; +++: synergism; - - - - -: very strong antagonism. +/-: no enhancement. Since SKNAS and F2112 were resistant to ABT263, an IC50 value for this compound was not reached. Therefore a combination index cannot be determined.

was observed in neuroblastoma cell line SKNAS, which lacks *BCL2* expression. Also exponentially growing human fibroblasts (F2112) did not show synergy (table 2), which indicates that the synergy is indeed *BCL2* dependent and tumor specific. The dose effect curve of SJNB12 treated with a concentration series of doxorubicin combined with a fixed concentration of ABT263 is represented in fig 5a. The isobologram of the combination of both compounds with various concentrations is shown in fig 5b. The Combination Index, which represents the degree of synergism of all drug combinations, is shown in table 2 for all cell lines tested. In this table the combination index at a fraction affected of 0.5 is shown (concentration combination

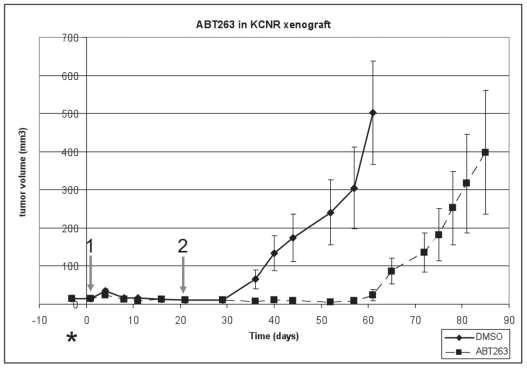

Figure 4: ABT263 in a KCNR xenograft model
The Y-axis represents tumor volume in mm3; the X-axis represents time in days after start of the treatment; * indicates the time point that tumor pieces were implanted; arrow 1 indicates the start of treatment and arrow 2 the end of the treatment. The solid line represents the average tumor volume of mice treated with DMSO; the dashed line represents the average tumor volume of mice treated with ABT263. From day 61 we had to terminate some mice in the control group because of large tumors.

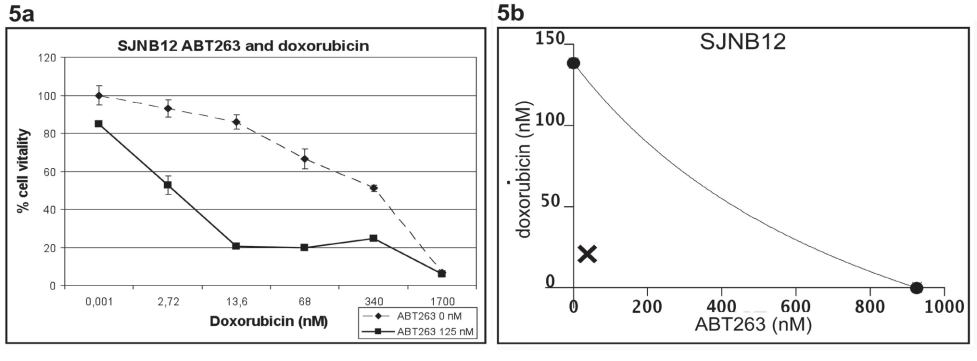

Figure 5: Synergy assays of ABT263 with doxorubicin in SJNB12
(A) the dose-effect curve of doxorubicin without ABT263 (dashed line) and with ABT263 (solid line). (B) Isobologram; The X-axis represents the concentration for ABT263 with a dot that represents its IC50 level. The Y-axis represents the concentration for doxorubicin, with a dot that represents its IC50 level. The line represents the expected curve for IC50 levels when both compounds are combined. X= actual concentrations of both drugs where an IC50 level was measured.

of compounds with 50% cell survival). However synergy was found at a large range of concentration combinations. These findings potentiate ABT263 for implementation in neuroblastoma treatment protocols and warrant further in vivo analysis.

Discussion

Neuroblastoma tumors have a very high *BCL2* RNA and protein expression, whereas the majority of neuroblastoma cell lines have not. Two cell lines (SJNB12 and KCNR)

show a *BCL2* expression that is comparable to the in vivo expression. Specific knockdown of *BCL2* with lentiviral shRNA resulted in the most abundant apoptotic response in these cell lines as shown by MTT assay and PARP cleavage. ABT263 synergistically sensitized neuroblastoma cell lines for most cytotoxic compounds. Treatment of neuroblastoma xenografts in a mouse model with ABT263 resulted in reduced and delayed tumor growth. We conclude that BCL2 is a potential new drug target in neuroblastoma and that further validation of the BCL2 inhibitor ABT263 in vivo and subsequently in patients is warranted.

Lestini et al[28] analyzed BCL2 and MCL1 protein expression on tissue arrays of neuroblastoma. Both proteins were expressed in the majority of neuroblastoma. Here we extend these observations by establishing that *BCL2* mRNA expression is much higher in neuroblastoma than in most other tumor types and normal tissues. In addition, we show that *BCL2* mRNA levels correlate very well with BCL2 protein levels as established by tissue arrays of tumors and western blot analysis of cell lines. Lestini et al. were successful in siRNA-mediated *BCL2* silencing in neuroblastoma cell lines, including SKNAS. In contrast to our SKNAS cells, their SKNAS cells showed BCL2 expression and knock-down, but just like our cells did not show an apoptotic response.

In other cancer models was also validated that sensitivity to BCL2 inhibition is dependent on levels of both pro- and anti-apoptotic members of the BCL2 family.[43,44] However, in neuroblastoma BCL2 is the only aberrantly expressed member of the BCL2 family, including the pro-apoptotic genes (data not shown). This indicates that BCL2 causes the unbalance in apoptosis and we think that the threshold of the BCL2 family members may be of importance. After inhibition of BCL2 the drop in BCL2 levels is big enough to induce apoptosis even though MCL1 is present.

ABT263 has previously been tested in a cell line panel by the Pediatric Preclinical Testing Program and relatively high IC50 values were found for the neuroblastoma cell lines tested.[31] *BCL2* expression has not been analyzed in these lines, but here we show that most neuroblastoma cell lines lack BCL2 expression, which might explain the weak responses to ABT263. The same holds for the neuroblastoma xenografts tested for ABT263 sensitivity as reported in the same paper. Also they were found to be relatively poor responders.

Essentially, our analyses showed that while neuroblastoma tumors have very high

BCL2 expression, most neuroblastoma cell lines have weak *BCL2* expression. Selection of high *BCL2* expressing cell lines for in vitro and in vivo testing of BCL2 inhibitory small molecules is therefore essential. The good responses in vitro and in vivo to ABT263 of neuroblastoma cell lines with high *BCL2* expression suggest that BCL2 might be a good target for therapy in neuroblastoma. Moreover, since the BCL2 expression in the selected cell lines is comparable to the BCL2 levels in most tumors, we expect that most tumors will be sensitive for ABT263.

Synergy of BCL2 inhibitors with etoposide or vincristine has previously been shown in other tumor types[39, 40]. We also found ABT263 to work synergistically with all of the currently used cytostatics in neuroblastoma treatment with the exception of cisplatin in SJNB12. The reason for this exception is unclear. For all other combinations, synergy could be explained by the working mechanisms of these compounds, which are all known to mediate DNA damage or microtubule destabilization. Cisplatin crosslinks DNA resulting in activation of DNA repair mechanisms and if that proves impossible it activates apoptosis. Doxorubicin is an inhibitor of reverse transcriptase and RNA polymerase, vincristin disrupts microtubules and etoposide blocks the cell cycle by inhibiting topoisomerase II.[41] All these mechanisms activate the mitochondrial apoptotic pathway.[42] This apoptotic route requires the release of Cytochrome C from the mitochondria, which is inhibited by BCL2.[2] Over-expression of *BCL2* therefore suppresses apoptosis and cells can be re-sensitized to these compounds by ABT263.

Combination treatment of ABT263 and currently used cytostatics might in addition increase the specificity of the anti-tumor treatment, as we show that *BCL2* is highly expressed in neuroblastoma but not in normal tissues. ABT263 is therefore a promising candidate for further in vitro testing and implementation in current treatment protocols of neuroblastoma patients.

Acknowledgements

This research was supported by grants from KIKA foundation, SKK and Netherlands Cancer Foundation. We would like to thank Thomas Klei and Lynne Rumping for their contribution.

Reference List

1. Yip, K.W. and Reed, J.C., Bcl-2 family proteins and cancer. Oncogene, 2008; 27**:** 6398-6406.
2. Frenzel, A., Grespi, F., Chmelewskij, W., and Villunger, A., Bcl2 family proteins in carcinogenesis and the treatment of cancer. Apoptosis, 2009; 14**:** 584-596.
3. Yecies, D., Carlson, N.E., Deng, J., and Letai, A., Acquired resistance to ABT-737 in lymphoma cells that up-regulate MCL-1 and BFL-1. Blood, 2010; 115**:** 3304-3313.
4. Egle, A., Harris, A.W., Bath, M.L., O'Reilly, L., and Cory, S., VavP-Bcl2 transgenic mice develop follicular lymphoma preceded by germinal center hyperplasia. Blood, 2004; 103**:** 2276-2283.
5. Vogler, M., Dinsdale, D., Dyer, M.J.S., and Cohen, G.M., Bcl-2 inhibitors: small molecules with a big impact on cancer therapy. Cell Death and Differentiation, 2009; 16**:** 360-367.
6. Zhang, L., Ming, L., and Yu, H., BH3 mimetics to improve cancer therapy; mechanisms and examples. Drug Resistance Updates, 2007; 10**:** 207-217.
7. Shoemaker, A.R., Mitten, M.J., Adickes, J., Ackler, S., Refici, M., Ferguson, D. et al, Activity of the Bcl-2 family inhibitor ABT-263 in a panel of small cell lung cancer xenograft models. Clinical Cancer Research, 2008; 14**:** 3268-3277.
8. Henry, M.C.W., Tashjian, D.B., and Breuer, C.K., Neuroblastoma update. Current Opinion in Oncology, 2005; 17**:** 19-23.
9. Maris, J.M., Hogarty, M.D., Bagatell, R., and Cohn, S.L., Neuroblastoma. Lancet, 2007; 369**:** 2106-2120.
10. van Noesel, M.M. and Versteeg, R., Pediatric neuroblastomas: genetic and epigenetic 'Danse Macabre'. Gene, 2004; 325**:** 1-15.
11. Maris, J.M., Medical Progress: Recent Advances in Neuroblastoma. New England Journal of Medicine, 2010; 362**:** 2202-2211.
12. Fesik, S.W., Promoting apoptosis as a strategy for cancer drug discovery. Nature Reviews Cancer, 2005; 5**:** 876-885.
13. Reed, J.C. and Pellecchia, M., Apoptosis-based therapies for hematologic malignancies. Blood, 2005; 106**:** 408-418.
14. Adida, C., Berrebi, D., Peuchmaur, M., Reyes-Mugica, M., and Altieri, D.C., Anti-apoptosis gene, survivin, and prognosis of neuroblastoma. Lancet, 1998; 351**:** 882-883.
15. Islam, A., Kageyama, H., Takada, N., Kawamato, T., Takayasu, H., Isogai, E. et al, High expression of Survivin, mapped to 17q25, is significantly associated with poor prognostic factors and promotes cell survival in human neuroblastoma. Oncogene, 2000; 19**:** 617-623.
16. Lamers, F., van der Ploeg, I., Schild, L., Ebus, M.E., Koster, J., Hansen, B.R. et al, Knockdown of Survivin (BIRC5) causes Apoptosis in Neuroblastoma via Mitotic Catastrophe. Endocrine Related Cancer, 2011;18(6):657-68.
17. Van Maerken, T., Ferdinande, L., Taildeman, J., Lambertz, I., Yigit, N., Vercruysse, L. et al, Antitumor Activity of the Selective MDM2 Antagonist Nutlin-3 Against Chemoresistant Neuroblastoma With Wild-Type p53. Journal of the National Cancer Institute, 2009; 101**:** 1562-1574.
18. Giaccone, G., Zatloukal, P., Roubec, J., Floor, K., Musil, J., Kuta, M. et al, Multicenter Phase II Trial of YM155, a Small-Molecule Suppressor of Survivin, in Patients With Advanced, Refractory, Non-Small-Cell Lung Cancer. Journal of Clinical Oncology, 2009; 27**:** 4481-4486.
19. Lewis, K.D., Samlowski, W., Ward, J., Catlett, J., Cranmer, L., Kirkwood, J. et al, A multi-center phase II evaluation of the small molecule survivin suppressor YM155 in patients with unresectable stage III or IV melanoma. Invest New Drugs, 2009.
20. Nakahara, T., Takeuchi, M., Kinoyama, I., Minematsu, T., Shirasuna, K., Matsuhisa, A. et al, YM155, a novel small-molecule survivin suppressant, induces regression of established human hormone-refractory prostate tumor xenografts. Cancer Research, 2007; 67**:** 8014-8021.
21. Satoh, T., Okamoto, I., Miyazaki, M., Morinaga, R., Tsuya, A., Hasegawa, Y. et al, Phase I Study of YM155, a Novel Survivin Suppressant, in Patients with Advanced Solid Tumors. Clinical Cancer Research, 2009; 15**:** 3872-3880.
22. Tolcher, A.W., Mita, A., Lewis, L.D., Garrett, C.R., Till, E., Daud, A.I. et al, Phase I and Pharmacokinetic Study of YM155, a Small-Molecule Inhibitor of Survivin. Journal of Clinical Oncology, 2008; 26**:** 5198-5203.
23. Lamers, F., Schild, L., Koster, J., Versteeg, R., Caron, H., and Molenaar, J. Targeted BIRC5 silencing using YM155 causes cell death in neuroblastoma cells with low ABCB1 expression. European Journal of Cancer, 2011; In Press.
24. Hoehner, J.C., Hedborg, F., Wiklund, H.J., Olsen, L., and Pahlman, S., Cellular Death in Neuroblastoma - In-Situ Correlation of Apoptosis and Bcl-2 Expression. International Journal of

Cancer, 1995; 62: 19-24.
25. Hoehner, J.C., Gestblom, C., Hedborg, F., Sandstedt, B., Olsen, L., and Pahlman, S., A developmental model of neuroblastoma: Differentiating stroma-poor tumors' progress along an extra-adrenal chromaffin lineage. Laboratory Investigation, 1996; 75: 659-675.
26. Hoehner, J.C., Hedborg, F., Eriksson, L., Sandstedt, B., Grimelius, L., Olsen, L. et al, Developmental gene expression of sympathetic nervous system tumors reflects their histogenesis. Laboratory Investigation, 1998; 78: 29-45.
27. Goldsmith, K.C., Lestini, B.J., Gross, M., Ip, L., Bhumbla, A., Zhang, X. et al, BH3 response profiles from neuroblastoma mitochondria predict activity of small molecule Bcl-2 family antagonists. Cell Death and Differentiation, 2010; 17: 872-882.
28. Lestini, B.J., Goldsmith, K.C., Fluchel, M.N., Liu, X.Y., Chen, N.L., Goyal, B. et al, Mcl1 downregulation sensitizes neuroblastoma to cytotoxic chemotherapy and small molecule Bcl2-family antagonists. Cancer Biology & Therapy, 2009; 8: 1587-1595.
29. Lin, T.S., New agents in chronic lymphocytic leukemia. Curr.Hematol.Malig.Rep., 2010; 5: 29-34.
30. Ackler, S., Xiao, Y., Mitten, M.J., Foster, K., Oleksijew, A., Refici, M. et al, ABT-263 and rapamycin act cooperatively to kill lymphoma cells in vitro and in vivo. Molecular Cancer Therapeutics, 2008; 7: 3265-3274.
31. Lock, R., Carol, H., Houghton, P.J., Morton, C.L., Kolb, E.A., Gorlick, R. et al, Initial testing (stage 1) of the BH3 mimetic ABT-263 by the pediatric preclinical testing program. Pediatric Blood & Cancer, 2008; 50: 1181-1189.
32. Fix, A., Lucchesi, C., Ribeiro, A., Lequin, D., Pierron, G., Schleiermacher, G. et al, Characterization of amplicons in neuroblastoma: High-resolution mapping using DNA microarrays, relationship with outcome, and identification of overexpressed genes. Genes Chromosomes & Cancer, 2008; 47: 819-834.
33. De Preter, K., Vandesompele, J., Heimann, P., Yigit, N., Beckman, S., Schramm, A. et al, Human fetal neuroblast and neuroblastoma transcriptome analysis confirms neuroblast origin and highlights neuroblastoma candidate genes. Genome Biology, 2006; 7.
34. Molenaar, J.J., Ebus, M.E., Koster, J., van Sluis, P., van Noesel, C.J.M., Versteeg, R. et al, Cyclin D1 and CDK4 activity contribute to the undifferentiated phenotype in neuroblastoma. Cancer Research, 2008; 68: 2599-2609.
35. Maurer, U., Charvet, C., Wagman, A.S., Dejardin, E., and Green, D.R., Glycogen synthase kinase-3 regulates mitochondrial outer membrane permeabilization and apoptosis by destabilization of MCL-1. Molecular Cell, 2006; 21: 749-760.
36. Yamamoto, K., Ichijo, H., and Korsmeyer, S.J., BCL-2 is phosphorylated and inactivated by an ASK1/Jun N-terminal protein kinase pathway normally activated at G(2)/M. Molecular and Cellular Biology, 1999; 19: 8469-8478.
37. Chou, T.C. and Talalay, P., Quantitative-Analysis of Dose-Effect Relationships - the Combined Effects of Multiple-Drugs Or Enzyme-Inhibitors. Advances in Enzyme Regulation, 1984; 22: 27-55.
38. Hagenbuchner, J., Ausserlechner, M.J., Porto, V., David, R., Meister, B., Bodner, M. et al, The Anti-apoptotic Protein BCL2L1/Bcl-xL Is Neutralized by Pro-apoptotic PMAIP1/Noxa in Neuroblastoma, Thereby Determining Bortezomib Sensitivity Independent of Prosurvival MCL1 Expression. Journal of Biological Chemistry, 2010; 285: 6904-6912.
39. High, L.M., Szymanska, B., Wilczynska-Kalak, U., Barber, N., O'Brien, R., Khaw, S.L. et al, The Bcl-2 Homology Domain 3 Mimetic ABT-737 Targets the Apoptotic Machinery in Acute Lymphoblastic Leukemia Resulting in Synergistic in Vitro and in Vivo Interactions with Established Drugs. Molecular Pharmacology, 2010; 77: 483-494.
40. Ackler, S., Mitten, M.J., Foster, K., Oleksijew, A., Refici, M., Tahir, S.K. et al, The Bcl-2 inhibitor ABT-263 enhances the response of multiple chemotherapeutic regimens in hematologic tumors in vivo. Cancer Chemotherapy and Pharmacology, 2010; 66: 869-880.
41. Imming, P., Sinning, C., and Meyer, A., Drugs, their targets and the nature and number of drug targets (vol 5, pg 821, 2006). Nature Reviews Drug Discovery, 2007; 6: 126.
42. Castedo, M., Perfettini, J.L., Roumie, T., Andreau, K., Medema, R., and Kroemer, G., Cell death by mitotic catastrophe: a molecular definition. Oncogene, 2004; 23: 2825-2837.
43. Moore, V.D., Brown, J.R., Certo, M., Love, T.M., Novina, C.D., and Letai, A., Chronic lymphocytic leukemia requires BCL2 to sequester prodeath BIM, explaining sensitivity to BCL2 antagonist ABT-737. Journal of Clinical Investigation, 2007; 117: 112-121.
44. Van Delft, M.F., Wei, A.H., Mason, K.D. et al, The BH3 mimetic ABT-737 targets selective Bcl-2 proteins and efficiently induces apoptosis via Bak/Bax if Mcl-1 is neutralized. Cancer Cell, 2006; 10: 389-399.

Supplementary Figures

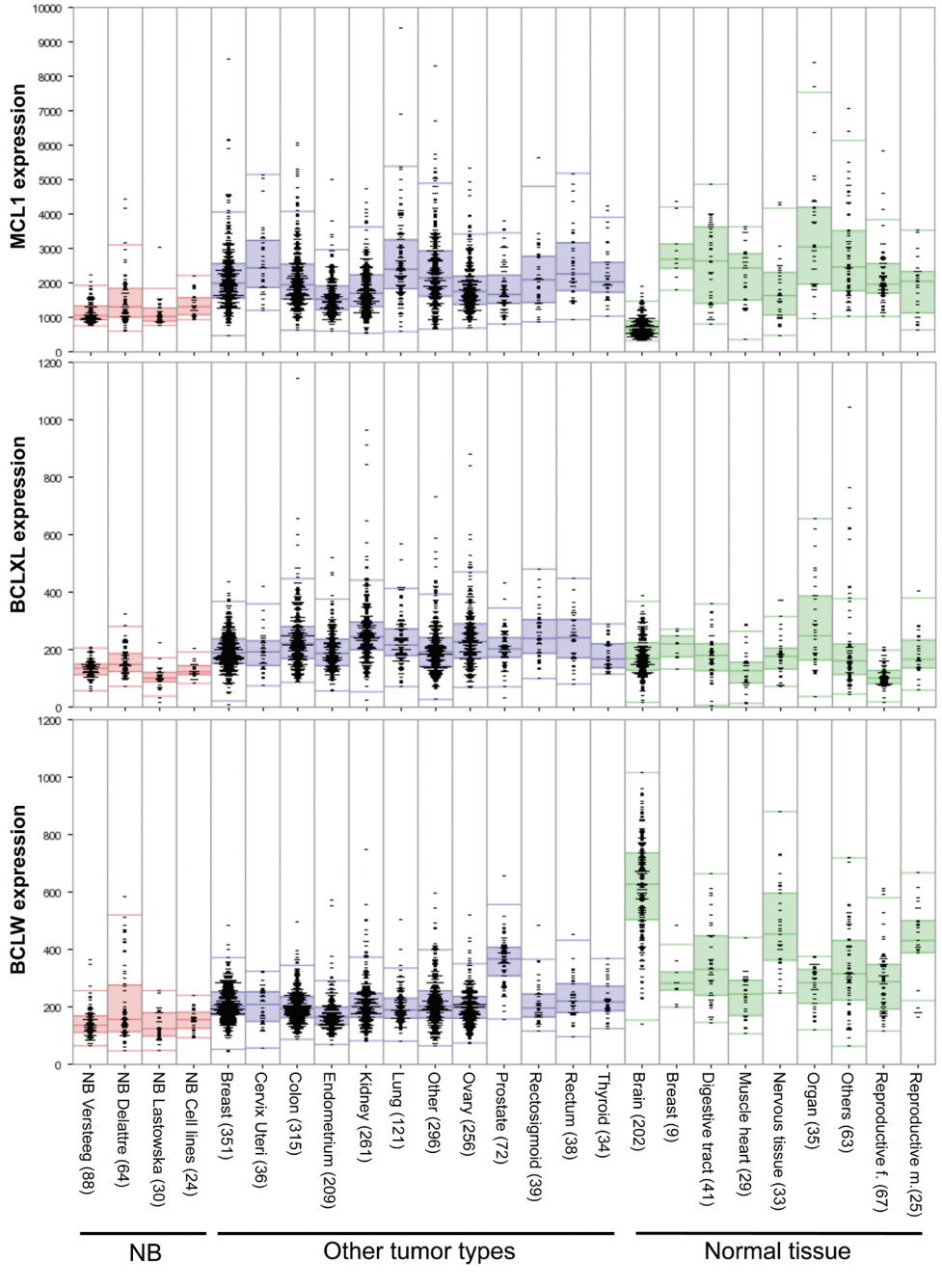

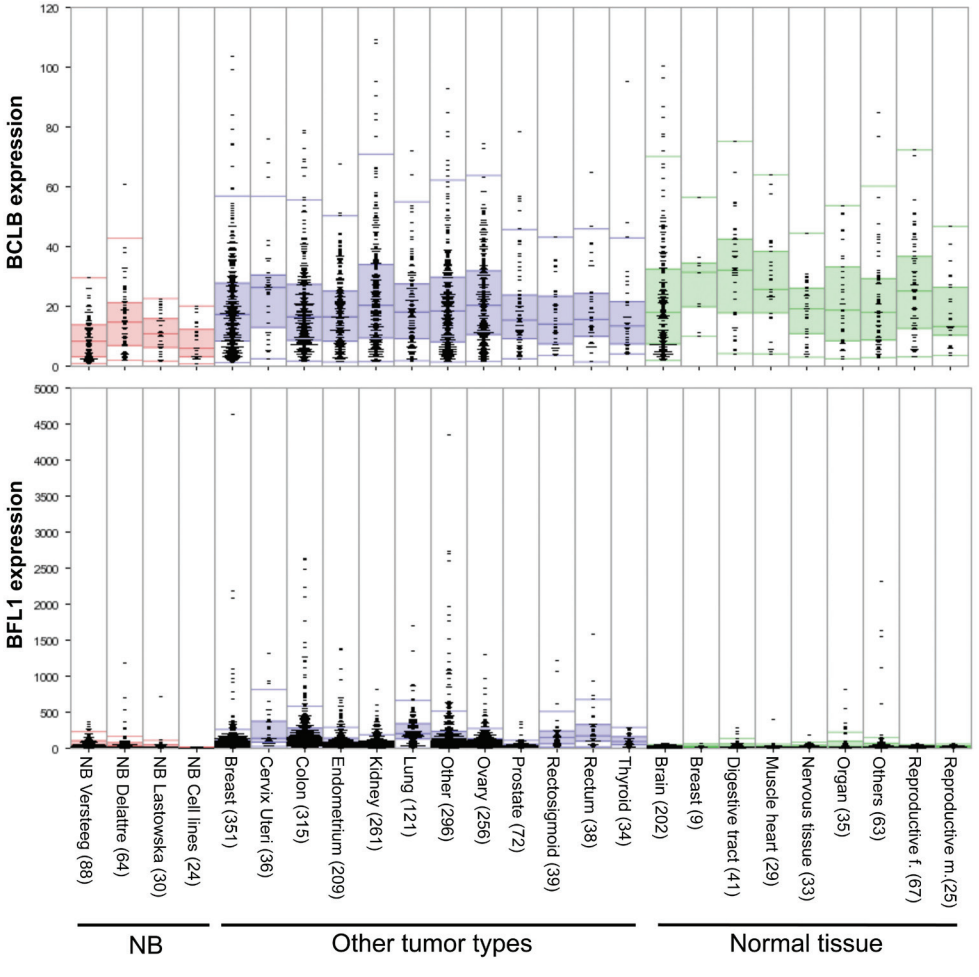

Supplementary figure 1/2. Expression of anti-apoptotic BCL2 family members in neuroblastoma tumors and cell lines

MCL1, BCLXL, BCLW, BCLB and BFL1 expression data in Neuroblastoma tumors and cell lines (red), other tumors (blue) and normal tissue (green) based on Affymetrix profiling. Every dot represents one sample; the number of tumor samples is given between brackets. The colored boxes represent the area between the 25th and the 75 percentile with a line in between indicating the median.

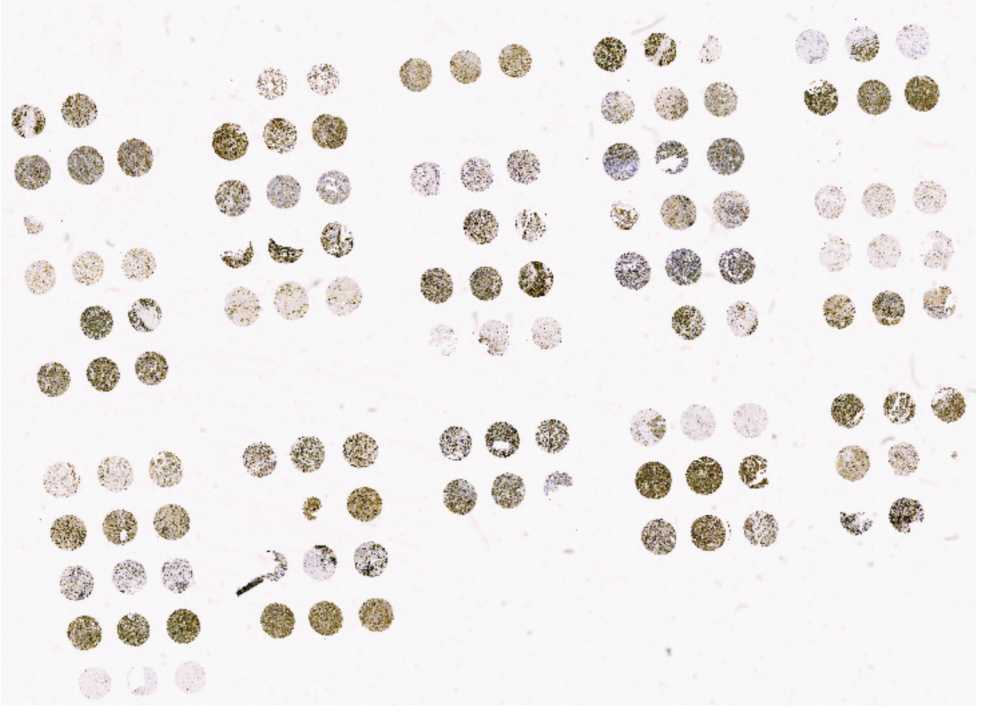

Supplementary figure 3. Tissue array of neuroblastoma tumors

Fig 1b is based on this tissue array. For each tumor 3 slides (shown next to each other) were stained.